

Implementation of MCEER TR 14-0006 Blast Load Curves in LS-DYNA[®] and Benchmark to Commonly Practiced Blast Loading Application Methods

Devon Wilson, Deborah Blass, and Sam Noli

Arup

Abstract

A tool has been developed to explore implementation of the blast load curves derived by J. Shin, A. Whittaker, A. Aref and D. Cormie in the MCEER Technical Report 14-0006 (2014). The MCEER proposed blast load curves capture the effects of high explosives near the face of the charge, where the traditionally-used Kingery and Bulmash (KB) empirical data is not applicable. Although not a replacement for a proper computational fluid dynamics assessment, designers can use simplified methods such as this tool to provide rough order of magnitude assessments prior to performing more complex and time intensive hydrocode methods.

*The ultimate intention of this tool is to supplement the capability of the current LS-DYNA method, *Load_Blast_Enhanced (LBE), which can then, if required, be used to complement more complex Arbitrary Lagrangian Eulerian (ALE) methods. It is not intended for this tool to replace the function of more sophisticated hydrocode methods.*

*The MCEER proposed curves for incident and reflected peak overpressures and impulses have been compared to *Load_Blast_Enhanced in range for validation before investigating the tool in the out-of-range values. The tool was developed to apply the polynomials into a calculation of load application to discrete elements in LS-DYNA based on the charge weight, standoff and angle of incidence geometry of the model.*

While the MCEER research provides values for calculating the pressure and impulse as angle of incidence varies, there exists a gap in published reflection coefficients for scaled distances less than 0.16 m/kg^{1/3}. A method for extrapolating the blast load curves has been assessed and a proposal for future research based on the findings is concluded.

Introduction

The use of polynomials derived from empirical data as published by Kingery and Bulmash (KB) in 1984 is widely established in industry to calculate blast loading on elements due to detonation of high explosives. Limitations of that data have also been widely known, primarily in limitations relating to what is commonly known as the "close-in" domain of explosions. The "close-in" domain occurs when the explosive detonates close enough to the structural element in consideration where complex gas expansion and wave effects would not have been captured in the empirical tests previously performed.

To help characterize this "close-in" domain, the concept of scaled distance, Z , is introduced below. Scaled distance, first formulated by B. Hopkinson (1915) and independently by C. Cranz (1926), states that similar blast waves are produced at identical scaled distances when two explosive charges of similar geometry and of the same explosive material but of different sizes, are detonated in the same atmosphere, according to the following equation:

$$Z = R / W^{1/3}$$

Where Z is the scaled distance, R is the standoff from the center of the charge to the face of the element being loaded, and W is the charge weight in TNT equivalence. J. Shin et al have loosely defined the "close-in" domain to be scaled distances $Z < 0.4 \text{ m/kg}^{1/3}$ (Shin 2014).

As noted earlier, data for far-field blast loading is widely available and has been validated more thoroughly throughout history than close-in detonations. This is partially due to instrumentation issues caused by the high pressures and temperatures in the close-in domain. This research aims to further a previously completed, relatively recent piece of analytical research to proposing new blast loading parameters in the close-in domain, *Air-Blast Effects on Civil Structures*, MCEER Technical Report 14-0006 (2014).

This research is not intended to review the accuracy of the previous MCEER work, but instead presents observations based on an evaluation completed from comparison between the newly proposed loading curves in the MCEER work and the widely recognized KB blast loading curves, using LS-DYNA. A Javascript tool has been written for an LS-DYNA preprocessor to implement the proposed MCEER loading into an LS-DYNA analysis so the curves can be reviewed in greater detail.

Background of Blast Load Calculation Methods

Multiple methods for calculating the air-blast loading parameters of high-explosives are available. The most notable in regard to high-explosives at a large range is based on the Kingery and Bulmash empirical data (1984). ConWep, a widely used software in the industry developed by the USAE Engineer Research & Development Center, incorporates the data from KB. Computational fluid dynamics (CFD) is also another method, by which there are various calculations algorithms. For the purposes of this research, CFD calculations have not been undertaken as CFD was the analysis method that was employed to derive the blast loading polynomials of the MCEER work. LS-DYNA additionally offers Arbitrary Lagrangian Eularian (ALE) as a tool for calculation blast loads, and more simply, *Load_Blast_Enhanced (LBE). A hybrid method of ALE and LBE, as well as particle methods are also available, but are less commonly used for structural analysis and are more computationally expensive methods, and therefore do not meet the intent of this research. The former, relevant methods are summarized in the below section.

Kingery & Bulmash / ConWep / *Load_Blast_Enhanced (LBE)

Kingery and Bulmash (KB) developed curves from empirical test data which have been widely adopted into U.S. government publications such as the TM 5-855-1 and the UFC 3-340-02. The curves have not been validated in the near field because pressure and temperatures are extremely high such that sensors are damaged as a result. Experimental results by which the KB curves were derived from were lacking within the near field domain. For example only four experiments with incident pressure-time histories at scaled distances less than $1.19 \text{ m/kg}^{1/3}$ were used, with no data for reflected pressures at scaled distances below $0.1 \text{ m/kg}^{1/3}$.

The computer code, ConWep (Hyde 1992) is a software developed by the USAE containing a collection of conventional weapons effects calculations from the equations and curves of TM 5-855-1, where the KB curves are implemented. Particularly relevant to this research, are the calculations for the aboveground airblast parameters, peak incident and reflected pressure and impulse, positive phase duration, and time of arrival. The calculations are based on the equations in TM 5-855-1, which are curve-fitted data based on the empirical tests performed by Kingery and Bulmash (1984).

*Load_Blast_Enhanced (LBE) is a calculation method in LS-DYNA by which the KB blast loading curves are applied. LBE assumes a Friedlander equation for the time-history loading function. LBE does not take into

account clearing effects, confinement effects, interaction of the blast wave with other structures or interference of the blast wave due to an object between the charge origin and the structure in question. LBE is an easy to use method for calculation of blast loading, but is only effective for idealized conditions where KB assumptions are also valid.

These methods are widely used in the industry for far-field detonations, but are limited in their use for near-field detonations. Scaled distance limitations for the positive phase duration are generally limited to a $0.147 \text{ m/kg}^{1/3}$ for spherical air-bursts and $0.178 \text{ m/kg}^{1/3}$ for hemispherical surface explosions. To perform blast analyses below these ranges, more expensive analyses methods such as computational fluid dynamics are typically undertaken.

Arbitrary Lagrangian Eulerian (ALE)

The ALE method is defined as the LS-DYNA Arbitrary Lagrangian Eulerian (ALE) solver paired with Fluid Structure Interaction (FSI) using `*CONSTRAINED_LAGRANGE_IN_SOLID` for fluid/structure mesh coupling. The ALE method takes the fluid mesh and performs a lagrangian step which deforms the mesh. Then an advection step is carried out to remap the distorted lagrangian mesh back on the original undeformed fluid (Eulerian) control volumes. This advection step can lead to the smoothing (dissipation) of rapid pressure changes (i.e. blast waves). The FSI method couples the fluid domain with the structural mesh. When a structural node is located in a fluid element a coupling force is applied to the node based on the fluid pressure. Conversely a pressure is also applied to the fluid to prevent it from flowing through the structure.

For blast loading, this methodology is carried out in practice by modelling the structure and, independently, a volume of air to sufficiently bound it. The creation or application of the blast wave can come from either a `*Load_Blast_Enhanced` (LBE) definition applied to a face of the air volume or the explicit modelling of explosive material that produces gas volumes and subsequent blast pressure waves via equations of state.

At large standoffs, the ALE method with explicitly modelled explosive is impractical as the small size of the elements required for the air becomes computationally too expensive. The hybrid analysis utilizing both LBE and ALE methods reduces that run time but the presence of the additional air elements as well as the `*Constrained_Lagrange_In_Solid` constraint definition is inherently more computationally expensive than a simple `*Load` based definition. Also, while an ALE approach captures the more complex behavior of the blast wave, including wrap around and shadowing, the complexity begets the need for more inputs (air properties, explosive properties, ALE controls etc.) and a deeper understanding of analytically modelling blast wave propagation.

Alternative Blast Load Mapping Approaches

Alternative blast pressure solvers, such as Air3D, can be utilized to develop pressure profiles that then can be input and applied to a LS-DYNA model.

Generally, the two-part nature of this analysis process and the conversion step to apply the loading into LS-DYNA create burdensome complexities especially if the process is not automated.

Air-Blast Effects on Civil Structures, MCEER Technical Report 14-0006 (2014) has researched blast load prediction of high explosives in both the far and near fields. The research compared a number of numerical CFD analyses performed in AUTODYN to the KB empirical data. After evaluation of the results, the MCEER paper has proposed new polynomials for predicting blast loads at scaled distances between 0.055 and 40 m/kg^{1/3}.

The authors performed numerical analyses using CFD to evaluate the shortcomings of the KB curves and to develop further blast loading data for use where the KB curves do not accurately predict the load. New proposed polynomials cover incident and normally reflected overpressure and impulse, as well as arrival time. Within the paper, the proposed polynomials are compared to the KB work as well as the CFD analyses undertaken within AUTODYN.

Two sets of polynomials are proposed, one which is applicable to the entire range of scaled distances between 0.055 and 40 m/kg^{1/3}, and another which has two parts where by the first part is applicable to the near-field range of scaled distances between 0.055 and 0.5 m/kg^{1/3} and the second part for scaled distances between 0.5 and 40 m/kg^{1/3}. In this manner, the authors suggest a method of use in the second set of polynomials whereby the near-field range of the KB curves can be replaced with the MCEER polynomials between 0.055 and 0.5 m/kg^{1/3}. The polynomials have been fitted similarly to the method used for KB, noting that higher order terms are required to accommodate the rapidly changing pressure and impulse values experienced in the near-field conditions.

The polynomials are of the form:

$$Y = C_0 + C_1U + \dots + C_NU^N$$

Where Y is the common logarithm of the blast parameter $U = K_0 + K_1 \cdot \log(Z)$, C and K are the constants proposed to fit the new polynomials, N is the order, and Z is the scaled distance.

The MCEER report suggests that the KB curves under predict incident and normally reflected peak overpressures and incident impulse near the face of the charge, at close ranges. Other major conclusions include:

- The MCEER study notes that the Friedlander equation is not valid for use in the near-field, recommending that CFD calculations must be used to accurately model the blast load time history in the near-field. The limit of the Friedlander equation is proposed to be $Z \geq 0.83 \text{ kg/m}^{1/3}$.
- UFC 3-340-02 under predicts values of incident peak overpressure, incident impulse and normally reflected peak overpressure for $Z < 0.08 \text{ kg/m}^{1/3}$, $0.1 \text{ kg/m}^{1/3}$, and $0.4 \text{ kg/m}^{1/3}$, respectively.
- UFC 3-340-02 overpredicts values of incident impulse for $0.1 \text{ kg/m}^{1/3} < Z < 40 \text{ kg/m}^{1/3}$ by 10 -20%.

Problem Statement

All the previously described methods used for calculations, with the exception of the MCEER work, have been reviewed and applied thoroughly in LS-DYNA. The MCEER report is a relatively new method which has not yet been widely rigorously studied or evaluated in academia or practice. Further, it has not yet been integrated into LS-DYNA for comparison to the other previously known methods.

Before the proposed polynomials are used in an analysis or design application in LS-DYNA, the new curves should be interrogated against other methods for blast loading calculation in LS-DYNA to have a better understanding of their impacts. To do this, the proposed MCEER polynomials requires a tool to translate the curves into a function applicable to LS-DYNA. Once a tool is created, the MCEER polynomial prediction of blast overpressures, impulses and arrival times can be benchmarked on the same platform using LS-DYNA against the older and established method of LBE.

This research is not to evaluate the validity of the proposed MCEER polynomials, but instead is a comparison of previous prediction methods to a new mathematical formulation using a common analysis tool, LS-DYNA. Observations during this process have been recorded.

Description of Tool

The implementation of the MCEER TR 14-0006 Blast Load Curves into LS-DYNA has been first implemented via a JavaScript “tool” created for Primer[®], a LS-DYNA pre-processor produced by Oasys Ltd. Through the JavaScript implementation, the application of the research found in the MCEER paper is able to be tested and validated before being hard-coded into LS-DYNA.

What follows is a description of the steps carried out to specify the inputs for the leading and then calculate and apply said loading. With eventual implantation within LS-DYNA directly, the inputs parameters would be specified in the cards of the newly created keyword and the loading calculation would application would occur internally in a manner similar to LBE.

On initiation of the JavaScript tool, the user is prompted to provide the following input:

- Detonation point (x, y, z coordinates)
- Mass of explosive (TNT equivalent)
- Selection of either a Spherical or Hemispherical blast wave
 - For a hemispherical wave, the equivalent TNT mass is scaled up by 1.8x
- A pre-defined segment set on which to apply the blast loading

With this input information provided, the tool is able to iterate through each of the segments in the desired set and perform the following suite of calculations:

1. Determine the nodes associated with the given segment
2. Determine the centroid of the segment
3. Calculate the distance from the blast origination point to the centroid of the segment (standoff)
4. Calculate the scaled distance for the segment based on the distance from Step 3 and the equivalent TNT input provided
5. Calculate the vector from the blast origination point to the centroid of the segment
6. Calculate the normal vector of the segment
7. Calculate the angle between the vectors in Step 5 and 6 (angle of incidence for the segment)
 - a. It should be noted that for the time being, segments with values greater than 90° are ignored as the functions are not applicable to wrap around conditions
8. The polynomial functions, with scaled distance and mass as inputs, are utilized to calculate the following:
 - a. Reflected Pressure
 - b. Incident Pressure

- c. Reflected Impulse
 - d. Incident Impulse
 - e. Time of Arrival
9. Using the angle of incidence and scaled distance in conjunction with both the pressure and impulse angle of incidence coefficient tables provided in the paper, bilinear interpolation is performed to obtain the precise angle of incidence coefficients for the peak pressure and impulse for the segment
 10. The pressure angle of incidence coefficient is multiplied by the Incident Pressure to obtain the actual peak pressure for the segment
 11. The impulse angle of incidence coefficient is multiplied by the Incident Impulse to obtain the actual impulse for the segment
 12. A generic Friedlander curve with a unit peak pressure and unit impulse is then used to populate a *DEFINE_CURVE card representing the pressure time-history
 13. The SFA (scale factor on the abscissa), SFO (scale factor on the ordinate), and OFFA (offset of the abscissa) on the *DEFINE_CURVE card are then updated such that the end manipulation to the unit Friedlander curve is a load curve that hits the peak pressure calculated in Step 10 at the time of arrival calculated in Step 8. The pressure returns to zero at a time such that the first integral of the curve is equal to the impulse calculated in Step 11
 14. Finally, a *LOAD_SEGMENT card is generated composed of the ID of the curve generated in Step 13 and the original segment nodes
 15. The process (Steps 1-14) is then repeated for the next segment in the desired set

In addition to creation of the required *LOAD_SEGMENT and *DEFINE_CURVE cards, two dummy shells are also created using *ELEMENT_SHELL_THICKNESS cards. The two shells use the segment nodes and are given a thickness equivalent to the peak pressure value and impulse value respectively.

The purpose of these two shell parts are for quick interrogation and visualization of the loads in the pre-processor. This is achieved by plotting the contour of the thickness of these parts individually to observe the pressure and impulse contour.

The intent of the tool is to provide an alternative blast wave loading calculation methodology for research and experimentation. Of particular interest is to test the response of structures at very close-in ranges where *LOAD_BLAST_ENHANCED and ConWep/Kingery & Bullmesh pressure and impulse calculations diverge.

The tool in its present form comes with the following limitations:

- The tool will not create a pressure curve and *LOAD_SEGMENT card for segments with an angle of incidence greater than 90°
 - The purpose of this is to limit the application of an inaccurate pressure time history to faces of the structure that would be shadowed from actually observing the full incident pressure
 - Future versions of the JavaScript tool as well as the code implemented in Dyna will allow users greater control on what surfaces with angles of incidence over 90° see the incident pressure/impulse. Care will be required from the user to apply the loading to only the appropriate surfaces (As with *LOAD_BLAST_ENHANCED)
- The accuracy of the reflected pressure, incident pressure, reflected impulse, incident impulse, and time of arrival are limited to the accuracy of the polynomials and the underlying research performed in the MCEER paper
- There is noted discrepancies when comparing the angle of incidence coefficients at 0° to the result of the reflected pressure or impulse divided by the incident pressure or impulse. While these two values

should theoretically be identical or nearly identical being that they there are by definition the same, there were moderate differences in values observed. This is likely due to differences that arise when fitting a curve with a polynomial. The handling of these differences will be explored further in the following section

Description of Extrapolation of the Angle of Incidence Coefficient Values for Close-In Scaled Distances

During the process of implementing the blast polynomials developed in the MCEER paper, it became clear that there was a gap in the research that was needed to fully and effectively bound the entire range of scaled distances (0.055 m/kg^{1/3} and greater) and angles of incidence (0°-90°). While the polynomials themselves provided reflected and incident pressure and impulse down to a scaled distance value of 0.055 m/kg^{1/3}, the angle of incident data provided in the paper covered only down to a scaled distance of 0.16 m/kg^{1/3}. When practically applying the research to a real-world scenario there exists an inability to calculate the loading for scaled distances less than 0.16 m/kg^{1/3}.

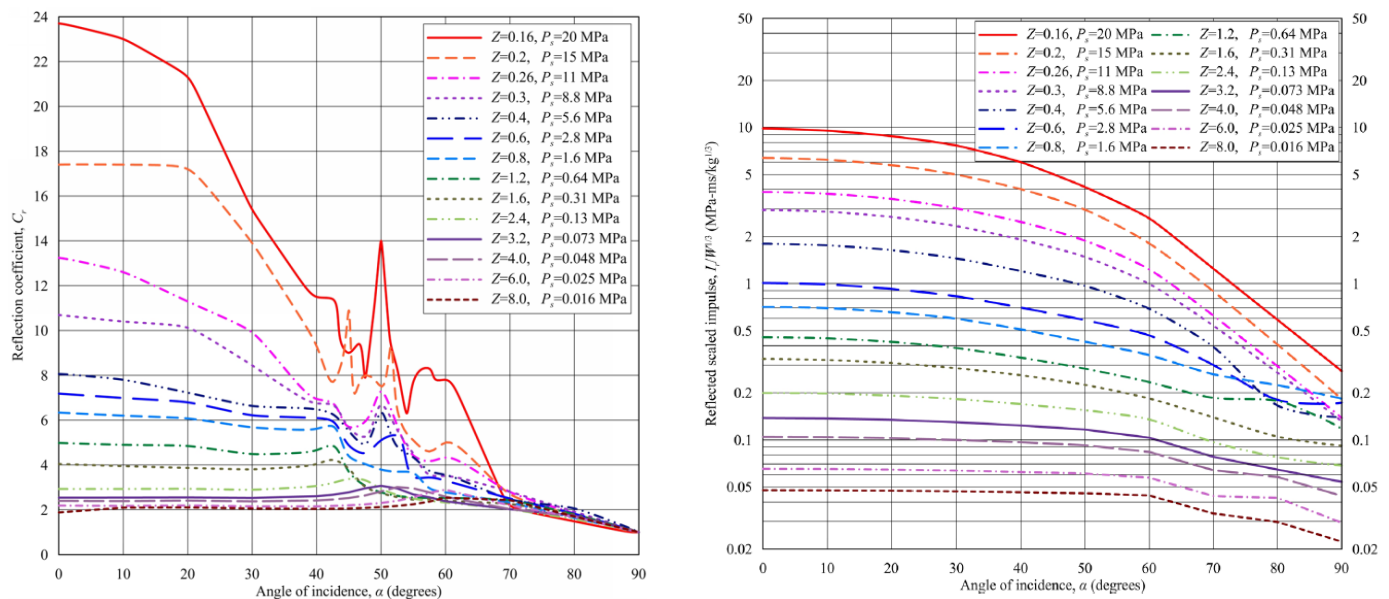


Figure 1 - Angle of incidence coefficient curves for Pressure (left) and Impulse (right) as derived by the MCEER research (Shin 2014)

An additional gap was noted when setting up the loading methodology. The calculation of the pressure and impulse is based on calculating the incident pressure and impulse and then applying the appropriate angle of incidence coefficient. As a result, for a segment that has an angle of incidence of zero, the reflected pressure is derived from factoring the angle of incidence even though the reflected pressure has been calculated in previous steps. The rationale for this is that for anything apart from an angle of incidence of exactly zero, the aforementioned methodology exists as the only means to calculate the pressure and impulse. Additionally, the occurrence of an angle of incidence of perfectly zero is exceedingly rare.

With that said, the methodology used is not in itself a limitation. Being that the angle of incidence coefficients and polynomials are derived from the same set of research it would be expected that the coefficient at 0 degrees would equal exactly the ratio of the calculated reflected pressure and impulse and incident pressure and

impulse. The exercise of comparison these two values was carried out for both pressure and impulse in Table 1 below. As can be seen, there exist reasonably significant percent differences (5-8% with a peak of 17%) between these two values for many of the scaled distances. This error is expected in some capacity as mathematical deviation is inevitable when polynomials are fit to a set of test data.

0° Angle of Incidence Coefficient - Pressure				0° Angle of Incidence Coefficient - Impulse			
Scaled Distance [Z]	0° Coefficient from MCEER Paper Curves	MCEER Polynomial Produced Coefficient [Cr=PR/PI]	Difference [%]	Scaled Distance [Z]	0° Coefficient from MCEER Paper Curves	MCEER Polynomial Produced Coefficient [Cr=PR/PI]	Difference (%)
0.055	-	15.12	-	0.055	-	15.12	-
0.08	-	61.79	-	0.08	-	61.79	-
0.12	-	41.81	-	0.12	-	41.81	-
0.16	23.70	25.08	5.84%	0.16	35.75	38.46	7.57%
0.20	17.40	17.24	-0.94%	0.20	35.00	37.76	7.88%
0.26	13.20	12.52	-5.14%	0.26	27.97	30.18	7.90%
0.30	10.70	10.36	-3.14%	0.30	22.60	24.27	7.41%
0.40	8.10	7.41	-8.57%	0.40	12.86	13.57	5.51%
0.60	6.90	6.53	-5.42%	0.60	5.84	6.04	3.47%
0.80	6.30	6.31	0.16%	0.80	3.87	4.02	3.80%
1.20	5.00	5.08	1.68%	1.20	3.85	3.71	-3.63%
1.60	4.00	4.05	1.31%	1.60	3.58	3.47	-3.18%
2.40	2.90	3.09	6.51%	2.40	2.88	2.91	1.00%
3.20	2.50	2.71	8.58%	3.20	2.56	2.59	1.07%
4.00	2.40	2.53	5.35%	4.00	2.39	2.42	1.21%
6.00	2.20	2.32	5.25%	6.00	2.17	2.23	2.59%
8.00	1.90	2.23	17.21%	8.00	2.18	2.13	-2.44%

Table 1 - Comparison of the 0° angle of incidence coefficient provided in the MCEER paper to the ratio of the MCEER polynomial produced reflected and incident pressure/impulse

While this percent difference introduces some uncertainty in the resulting pressure and impulse calculations, modification to the code was made to ensure that the pressure and impulse for a given scaled distance never exceed the reflected pressure/impulse. The logic being that the value calculated by the polynomials for the reflected pressure and impulse should always be the maximum achievable value even considering the Mach Stem phenomenon. The result of this modification can be observed in the example curve below for the pressures calculated at an arbitrary scaled distance (0.2370 m/kg^{1/3}). For angles of incidence lower than roughly 12 degrees, the angle of incidence coefficient multiplied by the incident pressure exceeds the reflected pressure. The pressure is thus capped at the reflected pressure value for angles in this range (i.e. the curve flattens at this ceiling value).

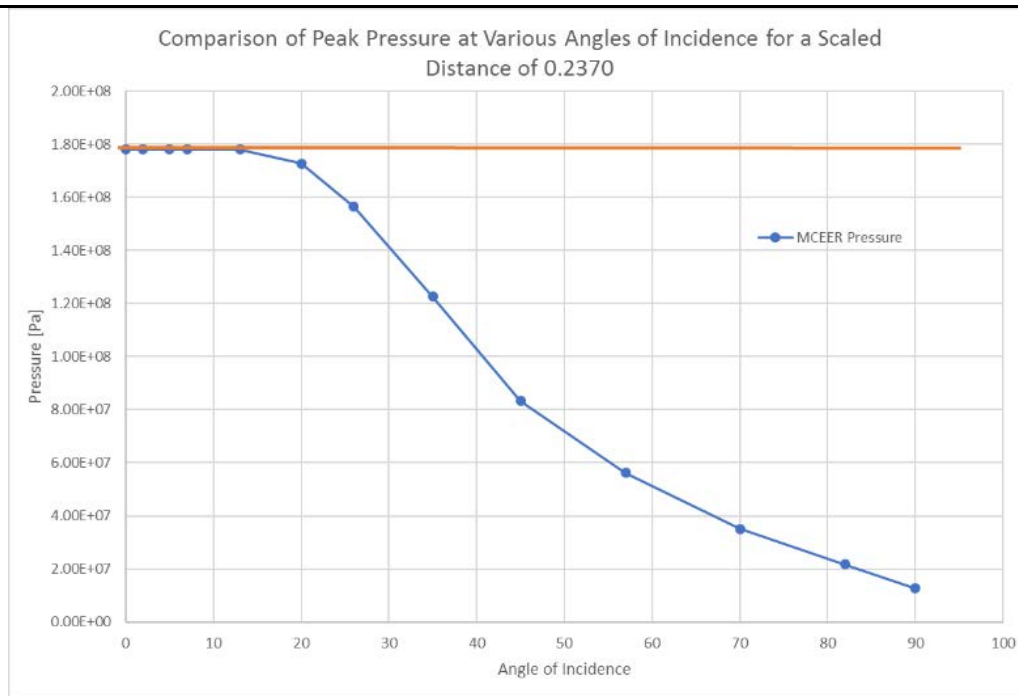


Figure 2 - Peak pressure calculated for various angles of incidence at an arbitrary scaled distance ($0.237 \text{ m/kg}^{1/3}$)

An effort was made to fill the gap in data detailed above (angle of incidence coefficients below $0.16 \text{ m/kg}^{1/3}$) all the while working under the constraint that is lack of access to the original research itself. This effort was carried out via a simple extrapolation of the angle of incidence coefficient curves into the desired range. The general approach for this extrapolation was to utilize the general shape of the lowest available curve ($0.16 \text{ m/kg}^{1/3}$). The curve was then scaled to the desired scaled distance utilizing two known points. The first is the 90° value which by definition is always 1. The second is the value at 0° and as before is equal to the ratio of the reflected and incident pressure/impulse. The $0.16 \text{ m/kg}^{1/3}$ scaled distance curve was scaled to fit these two end points. To get an accurate representation of the rapidly changing coefficients in the range between a scaled distance of 0.16 and $0.055 \text{ m/kg}^{1/3}$, two intermediate points ($0.12 \text{ m/kg}^{1/3}$ and $0.08 \text{ m/kg}^{1/3}$) were also utilized.

The angle of incidence coefficient curves for the impulse are all very regular at every scaled distance. As a result, the $0.16 \text{ m/kg}^{1/3}$ scaled distance curve is taken unmodified and scaled to the respective end levels for scaled distances of 0.12 , 0.08 , and $0.055 \text{ m/kg}^{1/3}$. It should be noted that for the data down to $0.16 \text{ m/kg}^{1/3}$, as the scaled distance decreased the coefficient curves steadily increased. Below $0.16 \text{ m/kg}^{1/3}$ though, the coefficient curves begin to drop significantly. This drastic change in this range highlights why the $0.16 \text{ m/kg}^{1/3}$ scaled distance curve could not be applied to all values below $0.16 \text{ m/kg}^{1/3}$.

The angle of incidence coefficient for the pressure is complicated slightly by the presence of Mach Stem. As can be seen in the MCEER paper's plot of angle of incidence coefficients, reproduced above in Figure 1, the values are volatile around the 50° mark. Based on the inability to carry out the research necessary to quantify the coefficient values for these lower scaled distances, a compromise was made. With the exception of the Mach Stem region, general shape of the coefficient curves for all scaled distances is very similar. As such, the $0.16 \text{ m/kg}^{1/3}$ scaled distance coefficient curve was first converted to a simplified version (dotted line). This simplified curve is then scaled in a fashion similar to the impulse coefficient curve. The results are plotted in Figure 3. As with the equivalent impulse curve, the three new extrapolated curves vary widely, illustrating the need to better quantify this range via the original research methodology.

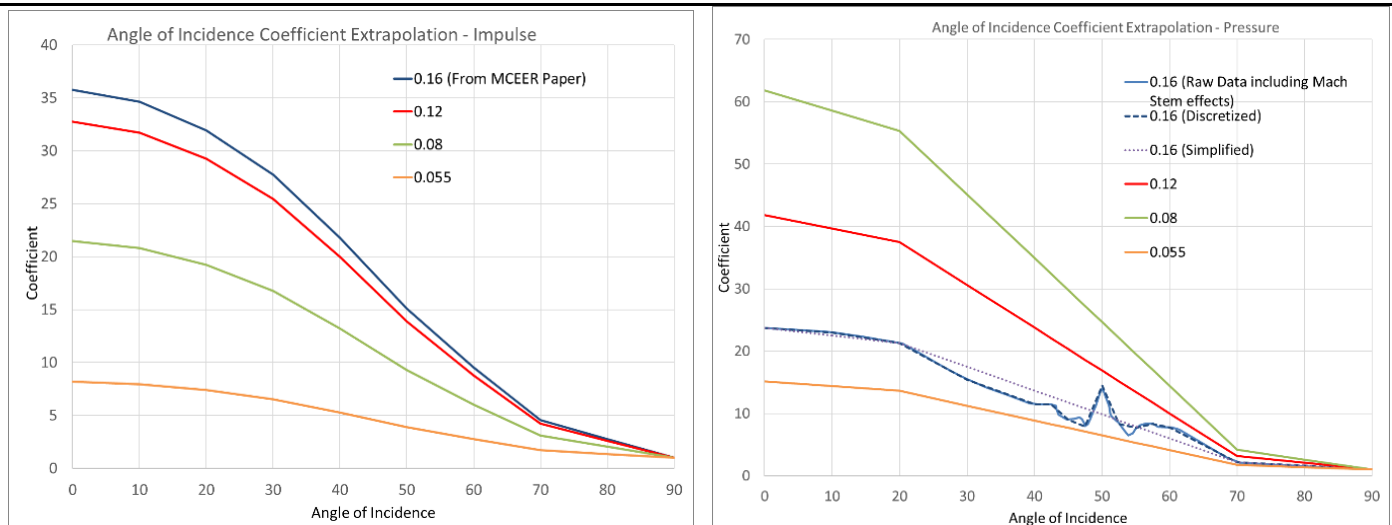


Figure 3 - Angle of incidence coefficient extrapolation for Impulse (left) and Pressure (right)

Comparison of MCEER Curves to Load Blast Enhanced

This section describes the validation models used for comparison of the blast loading curves and the results of the analyses performed.

The stated goal of implementing the MCEER polynomials into LS-DYNA is to benchmark pressure and impulse for very close-in distances against LBE. It is understood that LBE was not intended to be used in this range, however, for quick design assessments this was investigated to understand the level of difference. Reflected and incident results for Conwep/KB curves are also included for reference.

LS-DYNA Comparison Model

A comprehensive comparison model was developed to compare the pressures/impulses applied by the MCEER curves and those produced by the *LOAD_BLAST_ENHANCED keyword. The model consists of sets of square shells, each with a unit area, arranged at discrete locations along the Y axis with the goal of achieving a comprehensive distribution of scaled distance. At each location the group of shells are given varying angles with respect to the z-axis such that a comprehensive distribution of angles of incidence are achieved. Example images of the comparison model are shown in Figure 4. The scaled distances and angles of incidence that are considered in the comparison model are listed below in Table 2.

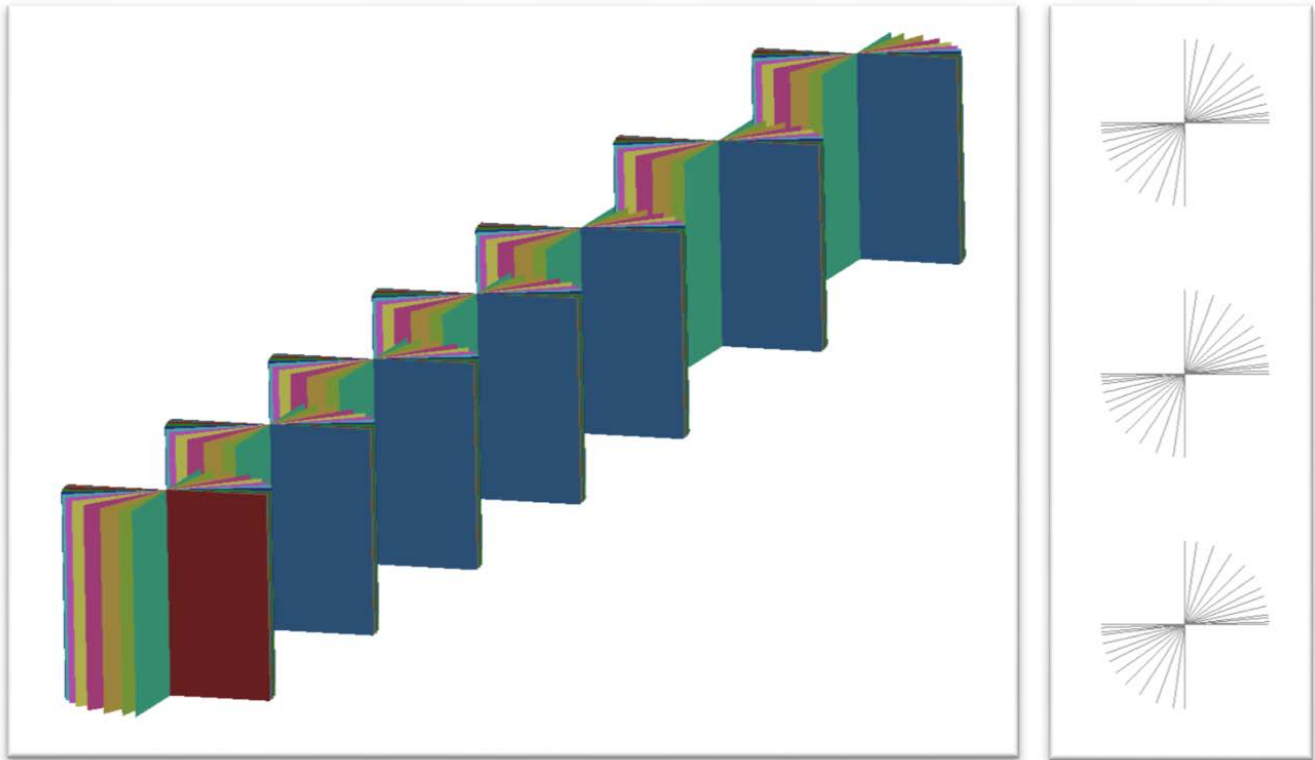


Figure 4 - Isometric (left) and top (right) views of comparison model

Comparison Model:	
Scaled Distances [m/kg ^{1/3}]	Angles of Incidence [Degrees]
0.0646	0
0.0969	2
0.1293	5
0.1616	7
0.1939	13
0.2370	20
0.2801	26
0.7110	35
1.1419	45
1.5727	57
2.0036	70
	82
	90

Table 2 - Ranges of Scaled Distance and Angle of Incidence considered in the comparison model

The comparison model was loaded separately with the MCEER derived loading (via the JavaScript tool) and *LOAD_BLAST_ENHANCED and each analyzed in LS-DYNA. Nodal Force Groups on each of the shells were utilized to extract individual force time histories for the shells. The force time histories were then divided by the shell area to arrive at pressure time histories. The pressure time histories were integrated to produce impulse time histories. The peak pressure and impulse from these sets of time histories were tabulated for

comparison. As reference, the incident and reflected pressure and impulse values were calculated from KB/ConWep and tabulated as well.

Results

The tabulated results for the six smallest scaled distance (the close-in area of interest) are shown in Table 3 and Table 4. The percent difference between the MCEER and LBE results are tabulated from pressure and impulse at all angles. In addition, the percent difference between KB /ConWep is shown for the 0° (reflected) and 90° (incident) angles.

The tabulated results are shown only for the close-in region as this is the area where deviation between the methodology occurs. Pressure and impulse values outside of this range match reasonably well for all three sources as documented in the MCEER paper. The full range is also documented in the pressure and impulse comparison curves that follow these tables. As can be seen in the tables, the pressure values are consistently much higher for the MCEER paper than LBE. Alternatively, the impulse difference between the MCEER paper and LBE varies considerably as the scaled distance increases. In particular, at a scaled distance of 0.1293 m/kg^{1/3}, the impulse derived by LBE is nearly double that derived by the MCEER paper polynomials. Referencing the KB/ConWep results at this scaled distance, we see a lower percent difference although it should be noted that the MCEER polynomial derived impulses vary by as much as ~50% at other scaled distance. Again, although LBE was not designed to be used in this area, the purpose of the research it to investigate the differences.

Scaled Distance [m/kg ^{1/3}]	Angle [deg]	MCEER		LBE		MCEER vs. LBE		K&B/ConWep		MCEER vs. K&B/ConWep	
		Pressure [kPa]	Impulse [kPa- msec]	Pressure [kPa]	Impulse [kPa- msec]	% Difference		Pressure [kPa]	Impulse [kPa- msec]	% Difference	
0.0646	0	4.09E+06	2.18E+05	5.357E+05	2.458E+05	87%	-13%	5.278E+05	2.45E+05	87%	-12%
	2	4.05E+06	2.17E+05	5.351E+05	2.455E+05	87%	-13%	-	-	-	-
	5	3.99E+06	2.15E+05	5.321E+05	2.442E+05	87%	-13%	-	-	-	-
	7	3.95E+06	2.14E+05	5.287E+05	2.426E+05	87%	-13%	-	-	-	-
	13	3.82E+06	2.07E+05	5.119E+05	2.349E+05	87%	-13%	-	-	-	-
	20	3.67E+06	1.96E+05	4.806E+05	2.206E+05	87%	-12%	-	-	-	-
	26	3.27E+06	1.82E+05	4.450E+05	2.043E+05	86%	-12%	-	-	-	-
	35	2.67E+06	1.54E+05	3.802E+05	1.747E+05	86%	-13%	-	-	-	-
	45	2.00E+06	1.18E+05	2.985E+05	1.373E+05	85%	-17%	-	-	-	-
	57	1.20E+06	7.57E+04	2.002E+05	9.245E+04	83%	-22%	-	-	-	-
	70	3.34E+05	3.70E+04	1.108E+05	5.156E+04	67%	-39%	-	-	-	-
82	2.08E+05	2.47E+04	5.814E+04	2.750E+04	72%	-11%	-	-	-	-	
90	1.24E+05	1.64E+04	4.340E+04	2.076E+04	65%	-26%	4.342E+04	8.63E+03	65%	47%	
0.0969	0	1.77E+06	1.19E+05	3.798E+05	1.731E+05	79%	-46%	3.740E+05	1.08E+05	79%	9%
	2	1.75E+06	1.18E+05	3.794E+05	1.729E+05	78%	-47%	-	-	-	-
	5	1.72E+06	1.17E+05	3.773E+05	1.719E+05	78%	-47%	-	-	-	-
	7	1.70E+06	1.16E+05	3.749E+05	1.708E+05	78%	-47%	-	-	-	-
	13	1.65E+06	1.12E+05	3.630E+05	1.654E+05	78%	-47%	-	-	-	-
	20	1.58E+06	1.06E+05	3.409E+05	1.554E+05	78%	-47%	-	-	-	-
	26	1.41E+06	9.78E+04	3.158E+05	1.440E+05	78%	-47%	-	-	-	-
	35	1.15E+06	8.24E+04	2.700E+05	1.233E+05	76%	-50%	-	-	-	-
	45	8.54E+05	6.17E+04	2.123E+05	9.718E+04	75%	-58%	-	-	-	-
	57	5.04E+05	3.80E+04	1.428E+05	6.567E+04	72%	-73%	-	-	-	-
	70	1.25E+05	1.62E+04	7.951E+04	3.697E+04	36%	-129%	-	-	-	-
82	6.99E+04	9.16E+03	4.220E+04	2.005E+04	40%	-119%	-	-	-	-	
90	3.31E+04	4.52E+03	3.167E+04	1.528E+04	4%	-238%	3.167E+04	3.84E+03	4%	15%	
0.1293	0	9.19E+05	6.70E+04	2.781E+05	1.269E+05	70%	-89%	2.741E+05	6.23E+04	70%	7%
	2	9.19E+05	6.66E+04	2.778E+05	1.268E+05	70%	-90%	-	-	-	-
	5	9.07E+05	6.60E+04	2.763E+05	1.261E+05	70%	-91%	-	-	-	-
	7	8.98E+05	6.56E+04	2.745E+05	1.253E+05	69%	-91%	-	-	-	-
	13	8.69E+05	6.34E+04	2.659E+05	1.214E+05	69%	-91%	-	-	-	-
	20	8.34E+05	5.99E+04	2.498E+05	1.141E+05	70%	-91%	-	-	-	-
	26	7.35E+05	5.52E+04	2.316E+05	1.058E+05	69%	-92%	-	-	-	-
	35	5.93E+05	4.65E+04	1.982E+05	9.074E+04	67%	-95%	-	-	-	-
	45	4.37E+05	3.46E+04	1.563E+05	7.173E+04	64%	-107%	-	-	-	-
	57	2.76E+05	2.11E+04	1.057E+05	4.879E+04	62%	-131%	-	-	-	-
	70	7.26E+04	8.64E+03	5.950E+04	2.788E+04	18%	-223%	-	-	-	-
82	4.39E+04	4.66E+03	3.217E+04	1.549E+04	27%	-233%	-	-	-	-	
90	2.47E+04	2.00E+03	2.434E+04	1.194E+04	1%	-496%	2.436E+04	2.16E+03	1%	-8%	

Table 3 – Comparison of MCEER pressure and impulse values to those derived by LBE for scaled distances of 0.0646, 0.0969, and 0.1293 m/kg^{1/3} (KB/ConWep shown for reference)

Scaled Distance [m/kg ^{1/3}]	Angle [deg]	MCEER		LBE		MCEER vs. LBE		K&B/ConWep		MCEER vs. K&B/ConWep	
		Pressure [kPa]	Impulse [kPa- msec]	Pressure [kPa]	Impulse [kPa- msec]	% Difference		Pressure [kPa]	Impulse [kPa- msec]	% Difference	
0.1616	0	4.58E+05	4.18E+04	2.101E+05	4.166E+04	54%	0%	2.078E+05	4.16E+04	55%	1%
	2	4.56E+05	4.16E+04	2.099E+05	4.162E+04	54%	0%	-	-	-	-
	5	4.52E+05	4.12E+04	2.087E+05	4.136E+04	54%	0%	-	-	-	-
	7	4.49E+05	4.09E+04	2.074E+05	4.108E+04	54%	0%	-	-	-	-
	13	4.36E+05	3.96E+04	2.009E+05	3.967E+04	54%	0%	-	-	-	-
	20	4.13E+05	3.74E+04	1.889E+05	3.705E+04	54%	1%	-	-	-	-
	26	3.45E+05	3.44E+04	1.752E+05	3.409E+04	49%	1%	-	-	-	-
	35	2.62E+05	2.90E+04	1.501E+05	2.868E+04	43%	1%	-	-	-	-
	45	1.75E+05	2.16E+04	1.186E+05	2.191E+04	32%	-1%	-	-	-	-
	57	1.57E+05	1.31E+04	8.058E+04	1.380E+04	49%	-5%	-	-	-	-
	70	4.34E+04	5.34E+03	4.585E+04	6.531E+03	-6%	-22%	-	-	-	-
82	2.91E+04	2.84E+03	2.519E+04	2.401E+03	13%	15%	-	-	-	-	
90	1.95E+04	1.17E+03	1.919E+04	1.439E+03	2%	-23%	1.943E+04	1.45E+03	1%	-24%	
0.1939	0	2.93E+05	2.91E+04	1.640E+05	3.031E+04	44%	-4%	1.622E+05	3.02E+04	45%	-4%
	2	2.93E+05	2.90E+04	1.638E+05	3.027E+04	44%	-4%	-	-	-	-
	5	2.93E+05	2.87E+04	1.629E+05	3.009E+04	44%	-5%	-	-	-	-
	7	2.93E+05	2.86E+04	1.619E+05	2.988E+04	45%	-5%	-	-	-	-
	13	2.93E+05	2.77E+04	1.569E+05	2.886E+04	46%	-4%	-	-	-	-
	20	2.90E+05	2.62E+04	1.475E+05	2.696E+04	49%	-3%	-	-	-	-
	26	2.54E+05	2.41E+04	1.369E+05	2.481E+04	46%	-3%	-	-	-	-
	35	1.93E+05	2.05E+04	1.175E+05	2.089E+04	39%	-2%	-	-	-	-
	45	1.31E+05	1.58E+04	9.308E+04	1.597E+04	29%	-1%	-	-	-	-
	57	8.50E+04	9.76E+03	6.355E+04	1.008E+04	25%	-3%	-	-	-	-
	70	4.27E+04	4.02E+03	3.654E+04	4.777E+03	14%	-19%	-	-	-	-
82	2.68E+04	2.11E+03	2.042E+04	1.789E+03	24%	15%	-	-	-	-	
90	1.63E+04	8.30E+02	1.567E+04	1.088E+03	4%	-31%	1.586E+04	1.09E+03	2%	-32%	
0.2370	0	1.78E+05	1.97E+04	1.225E+05	2.172E+04	31%	-10%	1.206E+05	2.15E+04	32%	-9%
	2	1.78E+05	1.96E+04	1.224E+05	2.170E+04	31%	-10%	-	-	-	-
	5	1.78E+05	1.95E+04	1.217E+05	2.157E+04	32%	-11%	-	-	-	-
	7	1.78E+05	1.94E+04	1.209E+05	2.142E+04	32%	-10%	-	-	-	-
	13	1.78E+05	1.88E+04	1.172E+05	2.069E+04	34%	-10%	-	-	-	-
	20	1.73E+05	1.78E+04	1.103E+05	1.934E+04	36%	-9%	-	-	-	-
	26	1.56E+05	1.64E+04	1.025E+05	1.781E+04	35%	-9%	-	-	-	-
	35	1.23E+05	1.40E+04	8.811E+04	1.501E+04	28%	-7%	-	-	-	-
	45	8.34E+04	1.10E+04	7.002E+04	1.151E+04	16%	-4%	-	-	-	-
	57	5.63E+04	7.04E+03	4.814E+04	7.302E+03	14%	-4%	-	-	-	-
	70	3.52E+04	3.00E+03	2.808E+04	3.511E+03	20%	-17%	-	-	-	-
82	2.17E+04	1.59E+03	1.603E+04	1.370E+03	26%	14%	-	-	-	-	
90	1.27E+04	6.44E+02	1.241E+04	8.599E+02	3%	-34%	1.241E+04	8.54E+02	3%	-33%	

Table 4 – Comparison of MCEER pressure and impulse values to those derived by LBE for scaled distances of 0.1616, 0.1939, and 0.2370 m/kg^{1/3} (KB/ConWep shown for reference)

Figure 5 and Figure 6 show the reflected pressure and reflected impulse as calculated by the MCEER paper and LBE as a function of scaled distance with the close-in region shown in detailed in the right-hand portion of the figure. Figure 7 and Figure 8 show the incident pressure and incident impulse as calculated by the MCEER paper and LBE as a function of scaled distance with the close-in region shown in detailed in the right-hand

portion of the figure. Figure 9 through Figure 11 show the peak pressure and impulse as a function of the angle of incidence for select close-in scaled distances.

As observed in the tabulated results, the MCEER polynomials derive consistently higher pressures than both LBE and KB/ConWep in the close range. Looking at the right hand sides of Figure 5 and Figure 6, the impulse produced by the MCEER polynomials appear to align well with KB/ConWep whereas LBE is a bit more erratic.

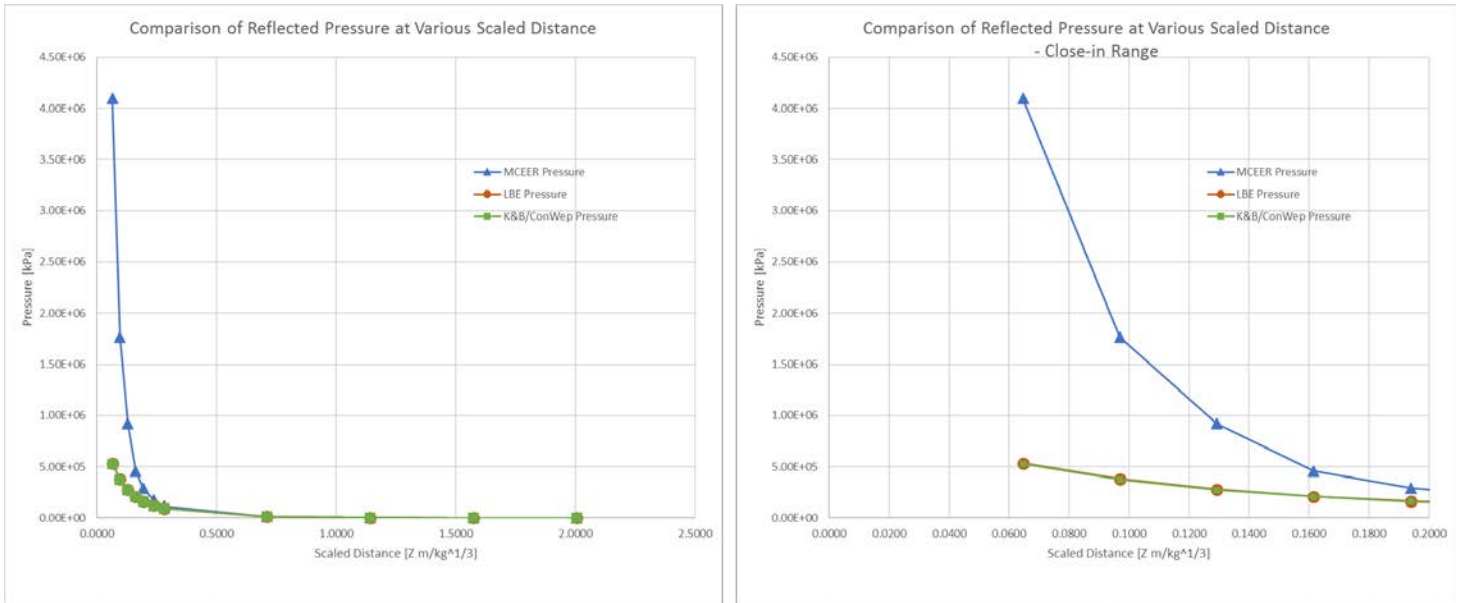


Figure 5 - Comparison of reflected pressure for a range of scaled distance values

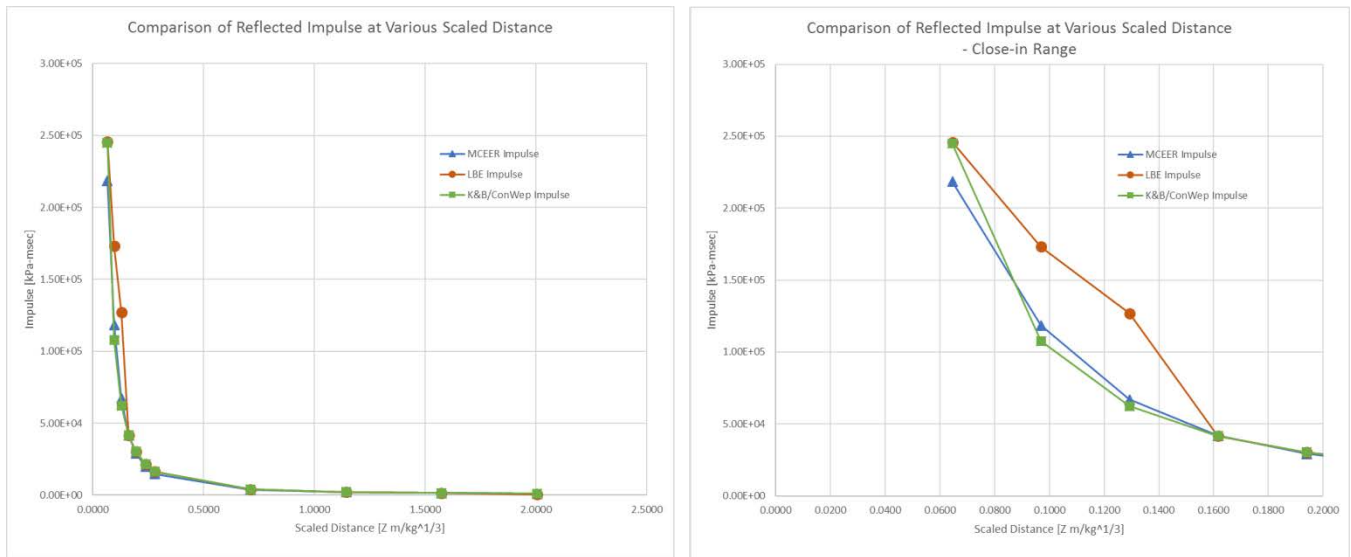


Figure 6 - Comparison of reflected impulse for a range of scaled distance values

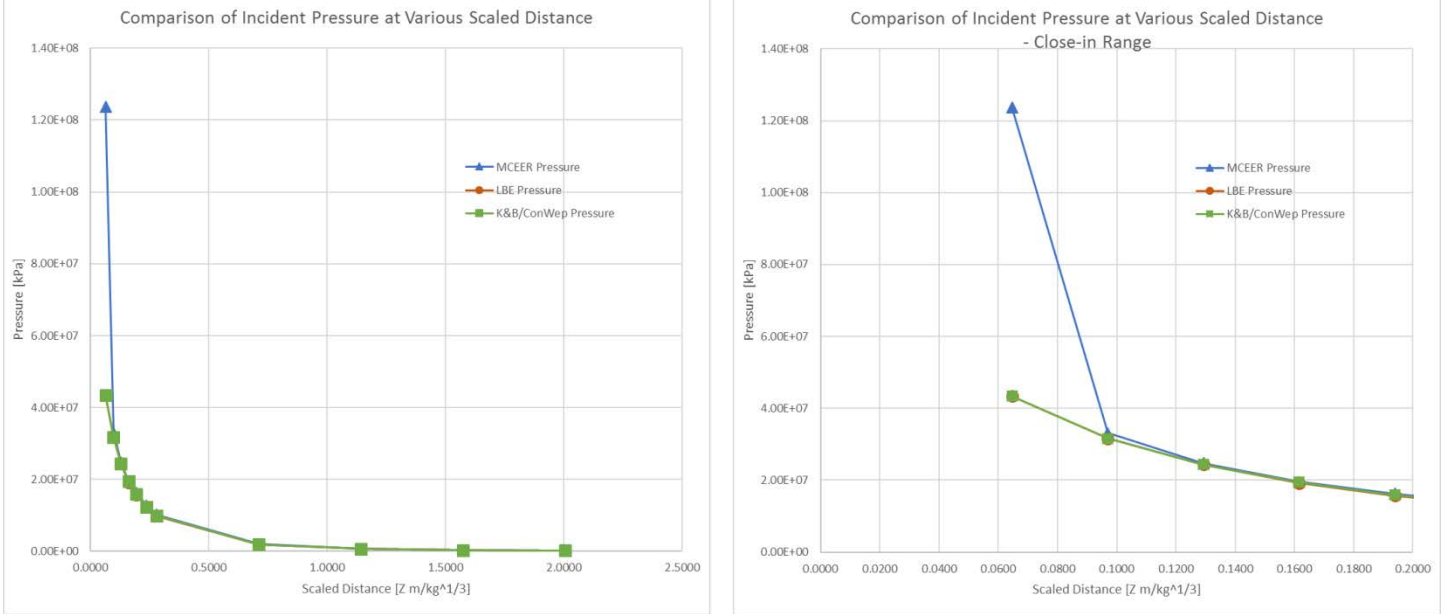


Figure 7 - Comparison of incident pressure for a range of scaled distance values

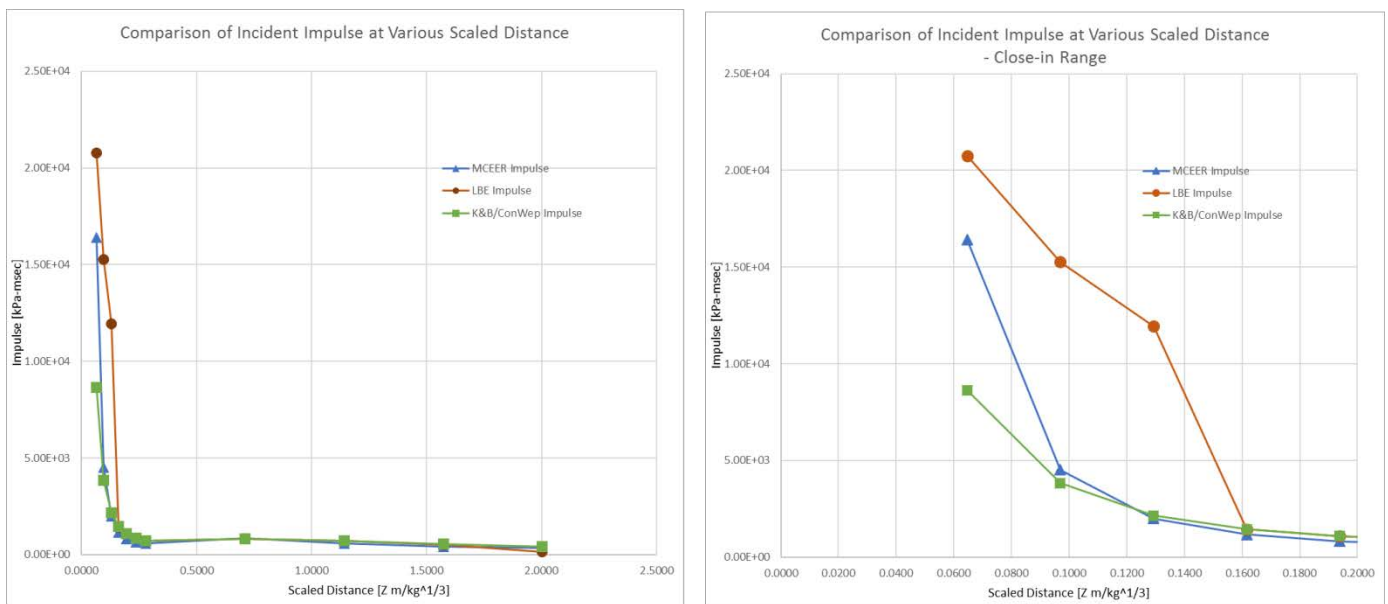


Figure 8 - Comparison of incident impulse for a range of scaled distance values

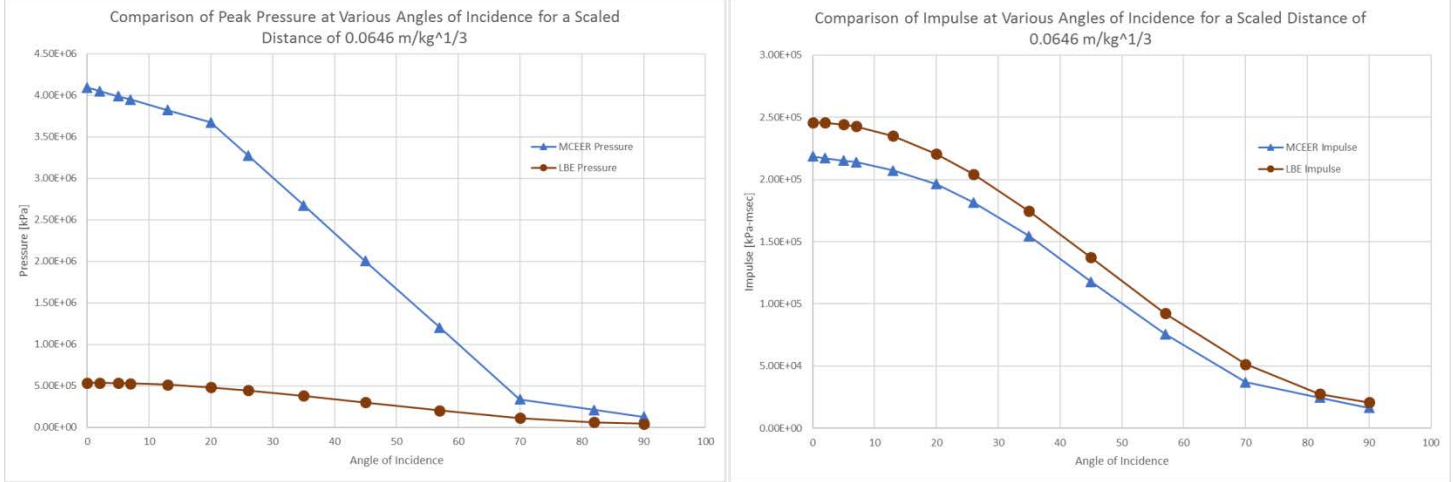


Figure 9 - Comparison of peak pressure for a range of angles of incidence ($Z=0.0646 \text{ m/kg}^{1/3}$)

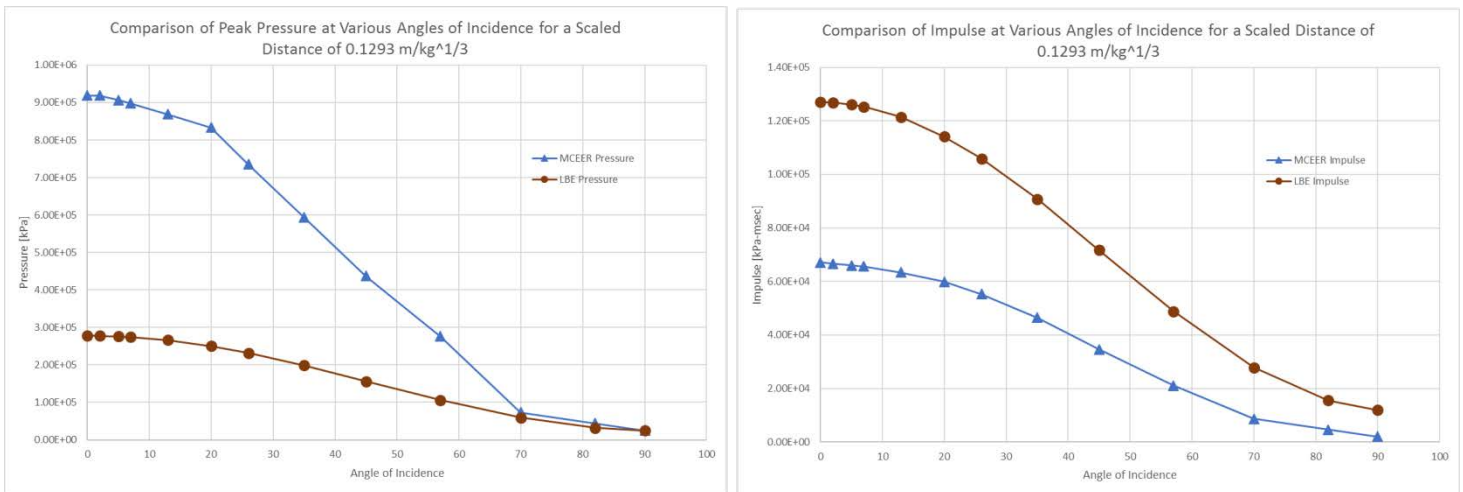


Figure 10 - Comparison of peak pressure for a range of angles of incidence ($Z=0.1293 \text{ m/kg}^{1/3}$)

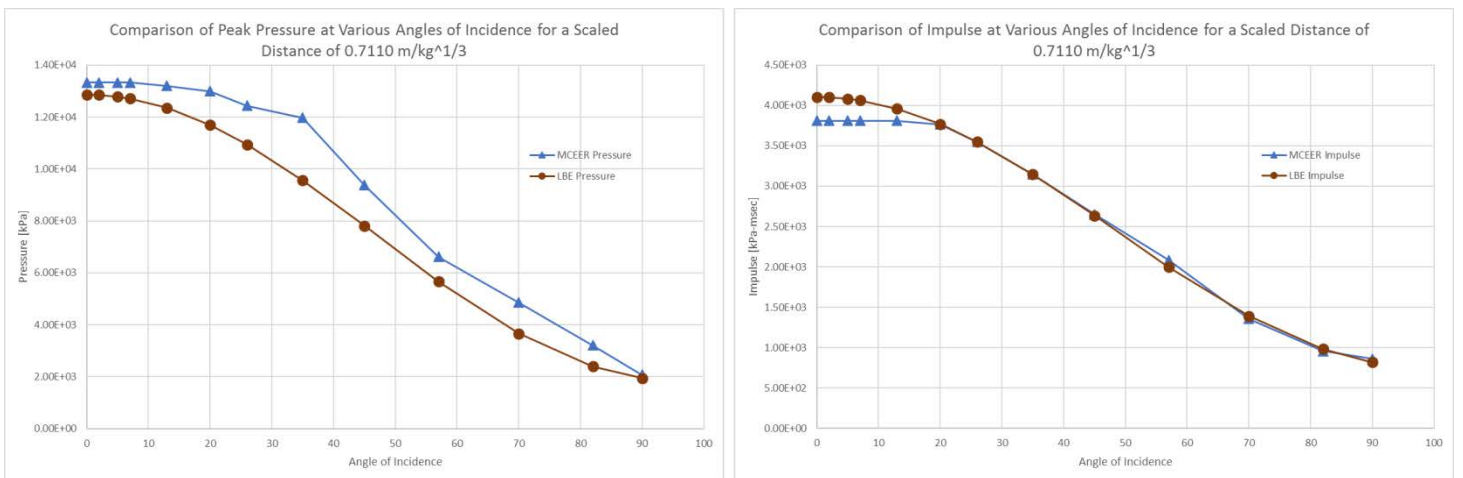


Figure 11 - Comparison of peak pressure for a range of angles of incidence ($Z=0.7110 \text{ m/kg}^{1/3}$)

Conclusions

The derivation of blast loads in the far field are typically undertaken within LS-DYNA using the LBE method, which is based upon KB curves. The new tool that has been introduced uses the research findings by MCEER, which enhances the work undertaken by KB, by providing revised polynomials to better calculate pressure and impulse associated with a TNT equivalent explosive charge in the near-field for various angle of incidences. For the far field, at varying angle of incidences, it uses analytically derived reflection coefficients. Near-field angle of incidence coefficients are omitted. In its current stage of development, the tool addresses this gap by adopting an interpolated process to calculate reflection coefficients for scaled distances less than $0.16 \text{ m/kg}^{1/3}$. Further research into analysis scenarios at varying angle of incidences are required to establish reflection coefficients at a scaled distance less than $0.16 \text{ m/kg}^{1/3}$. The tool correlates well in the far field with the existing KB curves. The tool is easy to implement, by allowing the user to select a segment set which blast pressures and durations are required.

There exists an opportunity to improve the tool by furthering the underlying MCEER research to produce precise angle of incidence coefficients for the very close in range of scaled distance ($0.16 \text{ m/kg}^{1/3}$ down to $0.055 \text{ m/kg}^{1/3}$). Additionally, further review of the angle of incidence curves as documented to ensure agreement with the underlying polynomials would be recommended.

The tool could be further developed to take into consideration simplistic clearing methods, such as those recommended within Chapter 2 of UFC 3-340-02. This would further enhance the objective of the tool to act as a preliminary analysis tool within the near-field domain. If additional accuracy is required for blast wave interaction with the environment hydrocode methods are recommended.

References

- Cranz, C., 1926. *Lehrbuch der Ballistik*, Springer-Verlag, Berlin.
- Hopkinson, B., 1915. "British Ordnance Board Minutes," 13565.
- Hyde, D. 2012, ConWep v. 2.1.1.1, USAE Engineer Research and Development Center
- Kingery, C. N. and Bulmash, G. 1984. Airblast parameters from TNT spherical air burst and hemispherical surface burst. *Report ARBRL-TR-02555*, US Army Ballistic Research Laboratory, Aberdeen Proving Ground, MD.
- LS-DYNA Keyword User's Manual, R9.0 (r:7883). Livermore Software Technology Corporation (LSTC): Livermore, CA 94551-5110, USA, August 2016
- Shin, J. et al. 2014, Air-Blast Effects on Civil Structures, MCEER Technical Report 14-0006, University at Buffalo, State University of New York.
- U.S. Department of Defense, Unified Facilities Criteria (UFC) 3-340-02 Structures to Resist the Effect of Accidental Explosions, 2014.
- U.S. Department of Defense, Army TMS-855-1 Design and Analysis of Hardened Structures to Conventional Weapons Effects, 1997.